NASA TECHNICAL NOTE

NASA TN D-4130

NASA TN D-4130

AERODYNAMIC HEATING IN THE VICINITY OF CORNERS AT HYPERSONIC SPEEDS

by P. Calvin Stainback and Leonard M. Weinstein

Langley Research Center
Langley Station, Hampton, Va.

NATIONAL AERONAUTICS AND SPACE ADMINISTRATION • WASHINGTON, D. C. • NOVEMBER 1967

NASA TN D-4130

AERODYNAMIC HEATING IN THE VICINITY OF CORNERS AT HYPERSONIC SPEEDS

By P. Calvin Stainback and Leonard M. Weinstein

Langley Research Center
Langley Station, Hampton, Va.

NATIONAL AERONAUTICS AND SPACE ADMINISTRATION

For sale by the Clearinghouse for Federal Scientific and Technical Information
Springfield, Virginia 22151 – CFSTI price $3.00

AERODYNAMIC HEATING IN THE VICINITY OF CORNERS AT HYPERSONIC SPEEDS*

By P. Calvin Stainback and Leonard M. Weinstein
Langley Research Center

SUMMARY

A study of hypersonic flow in a corner based on past experimental and theoretical studies and recent experiments has revealed at least three flow phenomena which influence the skin friction and heat transfer in the vicinity of a corner. The mutual interaction of the boundary layers in the corner results in a decrease in the local skin friction and heat transfer very near the corner. A vortex system and reattachment of the boundary layer downstream of shock-induced separation result in an increase in heating outboard of the mutual boundary-layer interaction region. Attempts to correlate the peak laminar heating in the vicinity of a corner and the location of this peak, in terms of local fluid properties, were partly successful for the simple models tested. It was found from limited data that the effect of the corner on the maximum increase in heating was less for a turbulent boundary layer than for a laminar boundary layer.

INTRODUCTION

The flow of a fluid in the vicinity of a corner formed by two intersecting surfaces is of interest since several types of corner configurations are encountered in the design of high-performance hypersonic aircraft. For example, they occur where the wing and control surfaces intersect the fuselage, where control surfaces intersect a wing, and in inlets. These corner-flow fields can influence the local skin friction and heat transfer to aircraft components and possibly alter the effectiveness of control surfaces. Because of these possible influences, the characteristics of these corner-flow regions should be investigated in order to determine their influence on overall vehicle performance.

Since most of the boundary layer over a high-performance hypersonic-cruise vehicle will probably be turbulent, it would be desirable to have data with fully developed turbulent flow in the corner region. Unfortunately, very few turbulent-flow data are available in corner regions at high Mach numbers since past interests were focused on high-altitude glide vehicles at conditions where

---

*Presented as Paper no. 17 at the classified "Conference on Hypersonic Aircraft Technology," Ames Research Center, May 16-18, 1967, and published in NASA SP-148.

laminar flow could be expected. Also, high Mach number facilities often have a limited maximum Reynolds number.

The purpose of the present paper is to review laminar-flow data obtained on various types of corner models, to present some recent laminar-flow heat-transfer data taken on simple corner models, and to present attempts to correlate peak laminar heating data for these simple models. Preliminary heat-transfer data will also be presented where there is a significant length of turbulent flow over a corner model. The turbulent results will be compared with the laminar results to indicate the effect of a turbulent boundary layer on peak heating in the vicinity of a corner. Although most of the results will be limited to heat-transfer data, some surface-flow visualization and flow-field visualization data will be presented.

SYMBOLS

h	aerodynamic heat-transfer coefficient
$h_{lam.th.}$	aerodynamic heat-transfer coefficient based on laminar theory
$h_{turb.th.}$	aerodynamic heat-transfer coefficient based on turbulent theory
M_∞	free-stream Mach number
N_{St}	Stanton number based on inclined surface fluid properties
$N_{St,max}$	maximum Stanton number based on inclined surface fluid properties
R_x, R_y, R_z	Reynolds number based on inclined surface fluid properties and on x, y, and z, respectively
R_∞	free-stream Reynolds number
r_n	nose radius
V_∞	free-stream velocity
x,y,z	coordinates
x_o	initial length (see fig. 1)
α	angle of attack
Λ	leading-edge sweep angle
ϕ	cant or rollout angle
ψ	yaw angle

REVIEW OF CORNER-FLOW PROBLEM

Corner flow has been a problem of interest in aerodynamics since the days of subsonic aircraft. However, at hypersonic speeds the corner-flow problem becomes much more complex as a result of the mutual intersection of shocks or shock—boundary-layer interactions or a combination of these phenomena. The corner-flow problem is not only complicated as a result of increased speed, but the many different geometries possible make the solution of the problem even more difficult. An example of some of the possible corner-flow configurations is shown in figure 1.

Several theoretical and experimental studies have been made by using one or a combination of the geometries shown in figure 1. These studies have revealed that at least three flow phenomena exist in and near corner regions. These phenomena are illustrated in figure 2.

From early theoretical studies by Loiziansky (ref. 1) and Loitsianskii and Bolshakov (ref. 2), a low-shear region was found to exist very close to the line of intersection between the two surfaces forming a corner. Later theoretical work by Bloom and Rubin (ref. 3) indicated that this low-shear region resulted in a low-heating region near the corner. Experimental pressure tests made by Bogdonoff and Vas (ref. 4) revealed a high-pressure region in the corner and a pressure distribution which they attributed to a vortex system generated by the leading edge of the corner. This high-pressure region was found to result in a high-heating region that was greater than could be attributed to the increase in pressure. (See ref. 5.) This increased heating tended to confirm the existence of the vortex system proposed by Bogdonoff and Vas. Flow surveys made by Cresci (ref. 6) using total-pressure and temperature probes probably give the best confirmation of the existence of a vortex system in the vicinity of the corner. Cresci states, however, that this vortex system exists within the boundary layer, a result which is in agreement with the theoretical results of Carrier (ref. 7). Further tests have been conducted to study vortex formations in the vicinity of a corner and these results will be presented subsequently.

Several investigators (Gulbran et al. (ref. 8) and Thomas (ref. 9), for example) noted that a sufficiently strong shock produced by one side of the corner or a blunt leading edge can cause the boundary layer to separate on the adjacent surface in the vicinity of the shock. This separation phenomenon could result in an increased heating at the point of reattachment. Therefore, it appears that there are two mechanisms which are responsible for increasing the heating in the vicinity of a corner: a vortex system and reattachment. A combination of these mechanisms is, of course, possible.

The influence of several factors on the peak heating found in the vicinity of a corner has been investigated. (For example, see ref. 10.) The results have indicated that some of the factors which increase peak heating in a corner region are increased Mach number, angle of attack, and nose radius; those factors which decrease peak heating are increased leading-edge sweep, cant or roll-out angle, and fillets.

From this review, it appears that previous investigations have resulted in a reasonable understanding of the laminar-flow mechanisms existing in a corner. Hopefully, for the present, this experience will be useful in gross predictions of surface heating and skin friction that will be encountered in a corner when the flow is turbulent. However, the level and possibly the extent of influences of corner phenomena on local surface conditions for the turbulent boundary layer would probably be different from those for the laminar boundary layer as a result of turbulent mixing.

RESULTS AND DISCUSSION

Laminar Corner-Flow Data and Correlation

Surface-flow visualization and heat-transfer data have been obtained on a simple corner model at a free-stream Mach number of 8 and a free-stream unit Reynolds number that ranged from 0.42×10^6 to 10×10^6 per foot. Flow-field visualization tests have also been conducted at a Mach number of 20 in helium with the use of the electron-beam technique.

Examples of the surface-flow visualization results are shown in figure 3. The model had an asymmetric angle of attack with one surface at an angle of attack of 5° and the other surface alined with the free-stream velocity. The data presented are for the alined surface. In the photograph showing the temperature-sensitive-paint results, the dark areas represent regions with higher heating rates than the light areas. The paint results indicate a series of low- and high-heating regions as the distance from the corner is increased. The low- and high-heating regions are seen to correspond to low- and high-shear regions as revealed by the oil-smear-technique results, also shown in the figure. The low- and high-shear regions revealed by the oil-flow results indicate the possible existence of separation (where oil accumulates) and reattachment (very light regions) in the regions of shock impingement. The large cross-flow component of some of the oil-flow lines revealed by the oil-dot technique also suggests the existence of a strong vortex system near the corner. Since it is difficult to distinguish between the influences of separation and reattachment and those of a vortex system by the use of surface-flow visualization techniques, an electron-beam technique has been used in a helium wind tunnel to visualize the flow field far from the surface. The electron beam injects a small beam of high-energy electrons into the test section flow which excites the helium atoms. The decay of these excited atoms produces a visible light in the flow field downstream of the beam. The light intensity is related to the local density of the flow field. An example of the results is shown in figure 4 where both surfaces are inclined 10° with respect to the free-stream velocity. The sketch in the upper left-hand section of the figure indicates the general location of the model in the tunnel, and the schematic drawing in the upper right-hand section indicates a part of the resultant flow field.

The photographs in the lower portion of figure 4 illustrate some of the preliminary results obtained up to the present time. The left-hand photograph

is a view from the rear of the model and below the level of the model surface; that is, the flow appears to be passing over the head of the observer. The electron beam reveals two types of flow structure in the left-hand photograph. First, a tear-drop-shaped dark region indicates the existence of one branch of a vortex system. The other structure, indicated by a light area extending from the corner at about 45° from either surface, is believed to be the resultant shock formed by the intersection of the two undisturbed wedge shocks. This type of intersection has been suggested by the low Mach number results of Charwat and Redekopp (ref. 11). In the right-hand photograph, the view is from the rear of the model and is directed parallel to the line of intersection of the two surfaces forming the corner. Note the small dark region which is again interpreted as being the core of one branch of a vortex system. Therefore, this is additional evidence that a vortex system exists in the vicinity of a corner for the present geometry.

Some typical heat-transfer results obtained with a corner model at an asymmetric angle of attack of $\alpha = 10^{\circ}$ and an angle of yaw of $\psi = 0^{\circ}$ is shown in figure 5. The data for the inclined surface indicate that there is a relatively low heating region near the corner caused by the mutual interaction of the boundary layers from adjacent surfaces. The heating rate increases as the distance from the corner is increased, reaches a peak, and ultimately decreases to the theoretical flat-plate value. The peak values of $N_{St}\sqrt{R_x}$ for various distances from the leading edge do not appear to be a function of x; therefore, the Stanton number for the peak heating would be expected to correlate as suggested by conventional flat-plate theory. Also, the peak values of $N_{St}\sqrt{R_x}$ are located at a given value of y/x. This fact indicates that the location of the peak heating is proportional to x.

The data for the alined surface (plotted on left-hand part of fig. 5) also indicate a low heating rate in the vicinity of the corner. The heating rate increases to a primary peak farther outboard and this location is nearer the corner than the projection of the shock from the inclined surface. Outboard of the primary peak, the heating decreases until a secondary increase in heating is formed outboard of the projected shock. Farther outboard of the secondary peak, the heating decreases to the theoretical flat-plate value. The Stanton and Reynolds numbers are based on properties for the inclined surface and result in the apparent low value of $N_{St}\sqrt{R_x}$ far from the corner on the alined surface.

It is interesting to note that for the alined surface the value of $N_{St}\sqrt{R_x}$ increases with increasing x; therefore, the peak heating data will probably not correlate in terms of N_{St} as a function of Reynolds number as suggested by the results for the inclined surface. The location of the peaks, however, appears to be at about a constant value of z/x and this fact indicates that z for the peak heating location is proportional to x.

Along the y/x and z/x axes of figure 5, the dark areas indicate regions in which oil remained on the model after the oil-flow tests, whereas the light areas indicate regions in which the oil was removed from the model by high shearing stresses. The peak heating rates are seen to occur where the shearing

stresses were also high. The combined oil-flow and heat-transfer results indicate the existence of a vortex system as shown by the curved arrows in figure 5.

Correlation of Laminar Peak Heating Data

Sample heat-transfer data have indicated the existence of peak heating rates on both of the surfaces that form a corner model. It would be desirable to correlate the magnitude of these peak heating rates and the location of their peaks. This information would be useful to design engineers if they encounter similar configurations in the design of practical high-performance hypersonic aircraft.

First, consider the data for the asymmetric corner where one surface is always alined with the free-stream velocity and the other surface has some inclination angle. The attempt to correlate these results for $\alpha = 0^\circ$, 5°, and 10° is shown in figure 6. Most of the data correlate fairly well with R_x, over a wide range of unit Reynolds numbers, until transition becomes apparent at high values of R_x. Some of the scatter present in the figure is due to the inability to define peak heating adequately as a result of the limited number of thermocouples near the leading edge of the model where peak heating is inboard of the thermocouples nearest the line of intersection. In general, the increase in heating ranges from about 50 to 65 percent above the laminar flat-plate theory of reference 12.

Since the data could be correlated in terms of the conventional viscous parameters, Stanton and Reynolds numbers, the peak heating rate on the inclined surface is apparently governed by viscous forces. This assumption appears reasonable since the shock produced by the alined surface is weak and probably would have negligible effect on the magnitude of the heating.

Although the present results for a Mach number of 8 and previous results from reference 5 for a Mach number of 5 indicate only a 50- to 65-percent increase in heating above theoretical flat-plate values for the $\alpha = 0^\circ$, $\psi = 0^\circ$ attitude, data taken at higher Mach numbers (M = 12 to 16, refs. 6 and 13) indicate a greater increase in the value of the peak heating - about 300 percent above laminar flat-plate theory. Therefore, it appears that the present correlations will probably be limited in usefulness up to a Mach number of about 8. However, when data become available at higher Mach numbers, the correlation parameters used herein might be applicable to the higher Mach number data.

The first attempt to correlate the data for the alined surface in terms of maximum Stanton number and Reynolds number is shown in figure 7. In this form, a satisfactory correlation was not obtained. Of course, this result was anticipated because of the results shown in figure 5 for the alined surface. It is interesting to note that the maximum Stanton number, for a given unit Reynolds number, is almost constant with Reynolds number for the limitations of the present model. This result has been noted before in reference 14 and is also in agreement with the data of reference 8. It is not clear at the present time why the Stanton number is constant with increasing Reynolds number. However, the peak-heating result is probably due to a combination of vortex system and

separation and reattachment. The invariance of the Stanton number with Reynolds number indicates that a strong inviscid phenomenon is probably controlling the peak heating on the alined surface.

Since the data did not correlate well with Stanton and Reynolds numbers, other parameters were tried in an attempt to obtain a better correlation. One such attempt is presented in figure 8. These parameters, $N_{St,max}/\sqrt{x}$ and R_x, appear to correlate the data fairly well. The use of the dimensional quantity x again indicates that inviscid flow mechanisms are important for this case where x would be the only scale parameter for purely inviscid flow.

The model was also tested with both surfaces having equal and positive inclination angles with respect to the free-stream velocity. For these data it was again found necessary to correlate the peak heating in terms of the parameters $N_{St,max}/\sqrt{x}$ and R_x. This correlation is shown in figure 9. Here again the correlation is fair, with much of the scatter due to inability to define adequately the peak heating near the leading edge. Transition appears to occur for this configuration at Reynolds numbers of about the same magnitude as for the inclined surface of figure 6.

It is interesting to note that when a strong shock crosses the instrumented surface it appears necessary to correlate the data in terms of the parameters $N_{St,max}/\sqrt{x}$ and R_x. As mentioned before, the use of the dimensional quantity x suggests that the peak heating is controlled by an inviscid flow phenomenon which is probably associated with the strong shock system. As pointed out previously, this phenomenon could be either a vortex system or separation and reattachment, or possibly both. Whether this type of correlation will be applicable for all geometries where strong shocks are generated must await further testing.

Correlation of the data for tests at negative angles of attack has been attempted, as shown in figures 10 to 14. For $\alpha = -5^\circ$ the correlations are fair, but for $\alpha = -10^\circ$ the data scatter to such an extent that no correlation exists for the parameters used. This scattering of the data could be due in part to the low heating rates experienced at negative angles of attack. Also, for the $\alpha = -5^\circ$, $\psi = -5^\circ$ case (fig. 14) the attempt to correlate the data was not successful.

Correlation of the Location of Laminar Peak Heating

The locations of laminar peak heating were correlated in the form of R_y or R_z as a function of R_x. These results are shown in figures 15 to 22. The correlations are fair for both surfaces of the model when any surface has a positive angle of attack, except at high Reynolds numbers where transition sometimes occurs. The slope of the correlation curves on log-log paper is about 1, which indicates that y or z is almost proportional to x for most of the range of the data. This prediction was indicated in figure 5.

The correlations were less successful at negative angles of attack (figs. 18, 19, and 22), and at $\alpha = -10^\circ$ (figs. 20 and 21) the scatter was so great that no correlation existed.

Effect of Cant Angle on Laminar Peak Heating

As pointed out in reference 10, several factors can reduce peak heating in the vicinity of a corner. Among these factors are increased leading-edge sweep, cant or rollout angle, and fillets. A second heat-transfer model was tested at a Mach number of 8 to investigate the effect of cant angle on peak heating in a corner. The instrumentation on this model was not as extensive as that on the model used to obtain the data previously discussed. The results of these tests for variation of the cant angle only are shown in figure 23. This figure reveals a substantial increase in peak heating resulting from reducing the angle between the plates from 90° to 60°. For example, the increase in peak heating for $\phi = 90^\circ$ is about 40 percent greater than that obtained from laminar flat-plate theory whereas the increase for $\phi = 60^\circ$ is about 80 percent greater. Of course, increasing the cant angle above 90° results in a decrease in peak heating until the angle reaches 180° (a flat plate). Further increase in ϕ to 270° (an exterior corner) results in little or no increase in heating above laminar flat-plate theory. The increase in peak heating with increasing x seen in figure 23 is apparently due to the limited number of thermocouples in this model. This fact makes it difficult to define peak heating near the leading edge of the model.

If the data obtained with the second model, for all cant angles except 90°, are compared with those obtained with the more completely instrumented first model ($\phi = 90^\circ$), it can be seen (fig. 24) that there is little or no increase in peak heating for $\phi = 60^\circ$ when compared with the heating for $\phi = 90^\circ$. However, the two larger values of ϕ ($\phi = 120^\circ$ and 270°) indicate a decrease in the level of peak heating when compared with the 90° case.

Turbulent Heating in the Corner Region

There is very little fully developed turbulent-flow data at high Mach numbers available in the literature for corner flow. However, since most of the flow over a hypersonic-cruise vehicle will probably be turbulent, a program has been undertaken to obtain fully developed turbulent-corner-flow data at a Mach number of 8. The models were constructed of glass-fused mica, and preliminary phase-change-paint data have been obtained with the model. Examples of some of the results obtained with this model are presented in figures 25 and 26. (See ref. 15 for discussion of phase-change paint.)

First consider only the data for the model with the sharp leading edges (fig. 25). The laminar-flow data (upper plot) reveal the characteristic low heating rate in the corner. The rate increases as the distance from the corner is increased, reaches a peak, and subsequently approaches flat-plate-theory values. The phase-change paint results at a Mach number of 8 indicate that for the same type of model with turbulent flow in the corner, there is no increase

in heating in the corner above turbulent theory. (See lower plot of fig. 25.) This was also true for the Mach number 5 data of reference 5.

When one of the surfaces has a blunt leading edge of 0.25 inch and data are recorded on the adjacent surface, the results shown in figure 26 are obtained. For the laminar-flow data (upper plot), the shock produced by the blunt leading edge results in a very large increase in heating on the adjacent surface. This increase can be about 12 to 13 times the laminar-flat-plate-theory value. (This increase is a function of x/r_n.) However, if the flow is turbulent outboard of the shock, the results shown in the lower portion of figure 26 are obtained. An increase in heating is noted above the turbulent-flat-plate-theory value in the turbulent-flow region as a result of shock impingement; however, this increase is only about 2.5 to 3 times the theoretical value.

From these preliminary results, it appears that the mechanisms which result in an increased peak heating in the vicinity of a corner for a laminar boundary layer are absent or greatly reduced in severity when the boundary layer is turbulent. This result is probably due to the well-known fact that a turbulent boundary layer is less sensitive to extraneous influences than a laminar boundary layer. This reduced sensitivity is, in turn, due to the turbulent mixing that fills out the velocity profile and thereby increases the average momentum of a turbulent boundary layer.

SUMMARY OF RESULTS

The results of the present study of flow in a corner at hypersonic Mach numbers can be summarized as follows:

1. A review of the literature and examination of the present data have revealed at least three flow phenomena existing in a corner which influence laminar skin friction and heat transfer to adjacent surfaces. The first of these phenomena is the mutual interaction between the two boundary layers on the surfaces forming the corner and the accompanying reduction of skin friction and heat transfer as a result of the interaction. The second is vortex systems generated by the corner-flow field and the increase in heating caused by these systems. The third is the separation and reattachment on one surface caused by strong shocks generated by the adjacent surface with an increase in heating at reattachment. The latter two phenomena often appear simultaneously.

2. Correlation of laminar peak heating and the location of the peak in terms of local fluid properties were partly successful for a limited range of corner geometries.

3. The limited amount of turbulent-flow data available indicates that the increase in peak heating in the vicinity of the corner will be less when the boundary layer is turbulent than when the boundary layer is laminar. This

result is probably due to the greater average momentum of a turbulent boundary layer so that it is less sensitive to extraneous influences than a laminar boundary layer.

Langley Research Center,
National Aeronautics and Space Administration,
Langley Station, Hampton, Va., May 17, 1967,
126-13-03-31-23.

REFERENCES

1. Loiziansky, L. G.: Interference of Boundary Layers. No. 249, Trans. Central Aero-Hydrodynamical Inst. (Moscow), 1936.

2. Loitsianskii, L. G.; and Bolshakov, V. P.: On Motion of Fluid in Boundary Layer Near Line of Intersection of Two Planes. NACA TM 1308, 1951.

3. Bloom, Martin H.; and Rubin, Stanley: High-Speed Viscous Corner Flow. J. Aerospace Sci., vol. 28, no. 2, Feb. 1961, pp. 145-157.

4. Bogdonoff, S. M.; and Vas, I. E.: A Preliminary Investigation of the Flow in a 90° Corner at Hypersonic Speeds. Part I - Flat Plate With Thin Leading Edges at Zero Angle of Attack. D143-978-013 (ARDC TR-59-202, AD 150 023), Bell Aircraft Corp., Dec. 20, 1957.

5. Stainback, P. Calvin: An Experimental Investigation at a Mach Number of 4.95 of Flow in the Vicinity of a 90° Interior Corner Alined With the Free-Stream Velocity. NASA TN D-184, 1960.

6. Cresci, Robert J.: Hypersonic Flow Along Two Intersecting Planes. PIBAL Rept. No. 895 (AFOSR 66-0500), Polytech. Inst. Brooklyn, Mar. 1966.

7. Carrier, G. F.: The Boundary Layer in a Corner. Quart. Appl. Math., vol. IV, no. 4, Jan. 1947, pp. 367-370.

8. Gulbran, C. E.; Redeker, E.; Miller, D. S.; and Strack, S. L.: Heating in Regions of Interfering Flow Fields - Part I. Two- and Three-Dimensional Laminar Interactions at Mach 8. Tech. Rept. AFFDL-TR-65-49, Pt. I, U.S. Air Force, July 23, 1965.

9. Thomas, John P.: Investigation of the Pressure Distribution on a Blunt-Fin Blunt-Plate Combination at a Mach Number of 11.26. ARL 66-0142, U.S. Air Force, July 1966.

10. Caldwell, A. L.; Haugseth, E. G.; and Miller, D. S.: The Influence of Aerodynamic Interference Heating on Directional Stability Problems of Hypersonic Vehicles. Paper 63-6, Inst. Aerospace Sci., Jan. 1963.

11. Charwat, A. F.; and Redekopp, L. G.: Supersonic Interference Flow Along the Corner of Intersecting Wedges. AIAA J., vol. 5, no. 3, Mar. 1967, pp. 480-488.

12. Cohen, Nathaniel B.: Boundary-Layer Similar Solutions and Correlation Equations for Laminar Heat-Transfer Distribution in Equilibrium Air at Velocities up to 41,000 Feet Per Second. NASA TR R-118, 1961.

13. Miller, D. S.; Hijman, R.; Redeker, E.; Janssen, W. C.; and Mullen, C. R.: A Study of Shock Impingements on Boundary Layers at Mach 16. Proc. 1962 Heat Transfer and Fluid Mech. Inst., F. Edward Ehlers, James J. Kauzlarich, Charles A. Sleicher, Jr., and Robert E. Street, eds., Stanford Univ. Press, 1962, pp. 255-278.

14. Bertram, Mitchel H.; Fetterman, David E., Jr.; and Henry, John R.: The Aerodynamics of Hypersonic Cruising and Boost Vehicles. Proceedings of the NASA-University Conference on the Science and Technology of Space Exploration, Vol. 2, NASA SP-11, 1962, pp. 215-234. (Also available as NASA SP-23.)

15. Jones, Robert A.; and Hunt, James L.: Use of Fusible Temperature Indicators for Obtaining Quantitative Aerodynamic Heat-Transfer Data. NASA TR R-230, 1966.

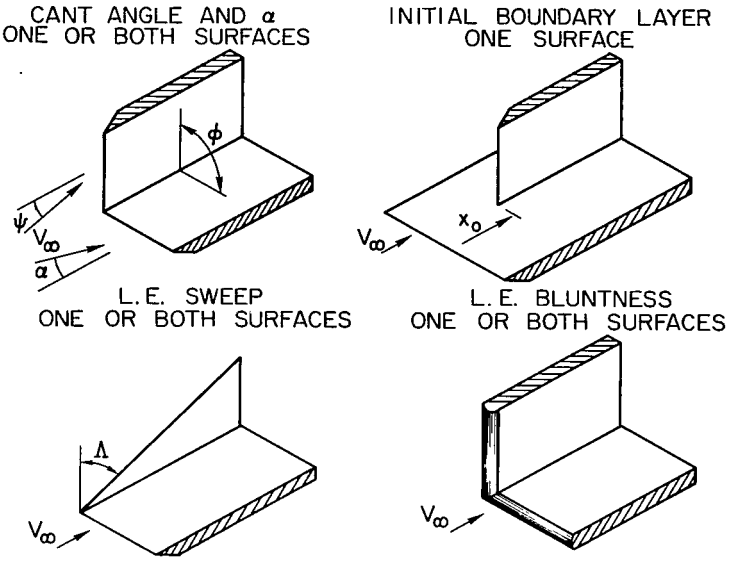

Figure 1.- Corner-flow configuration.

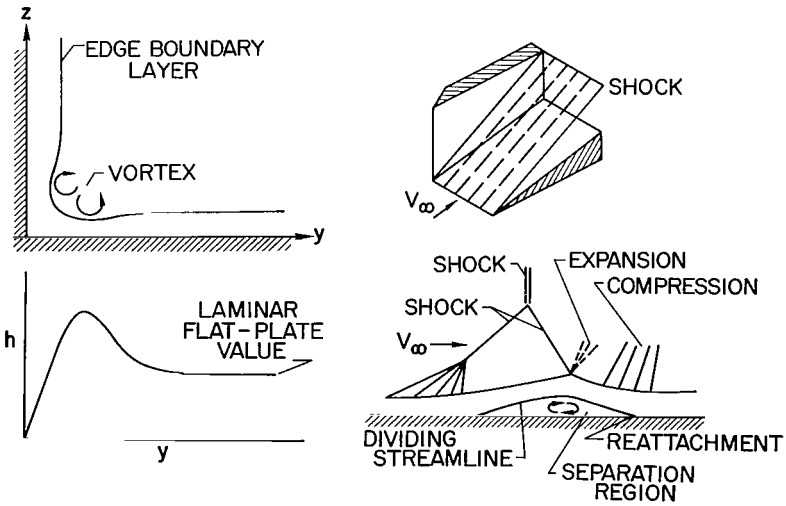

Figure 2.- Flow phenomena in a corner.

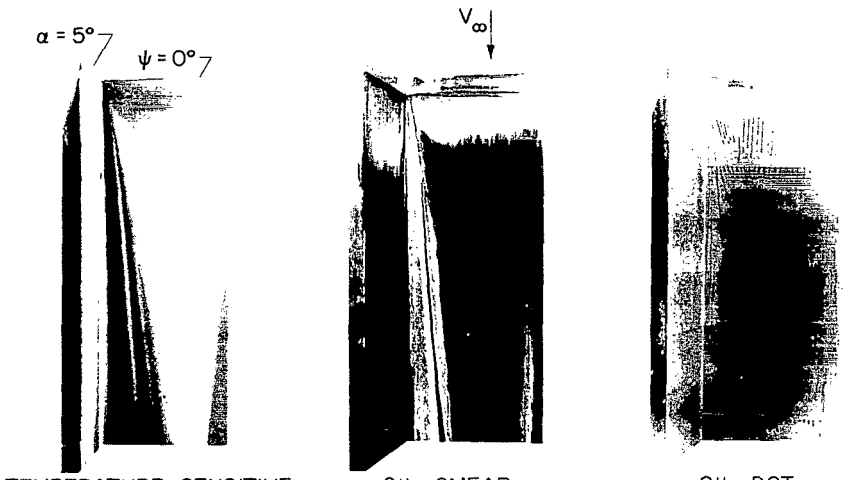

Figure 3.- Surface-flow visualization in a corner. $M_\infty = 8$; $R_\infty/ft = 3.15 \times 10^6$.

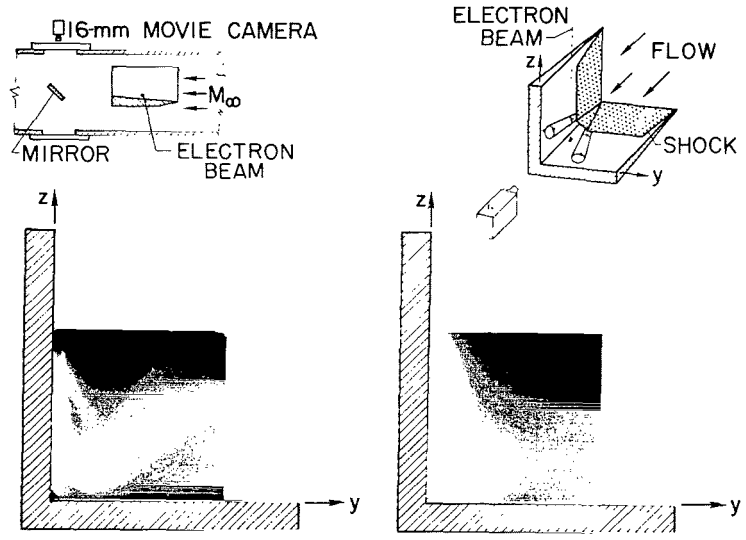

Figure 4.- Electron-beam corner-flow visualization. $M_\infty = 20$ in helium; $R_\infty/ft = 4.56 \times 10^6$; $\alpha = 10°$; $\psi = 10°$; $\phi = 90°$.

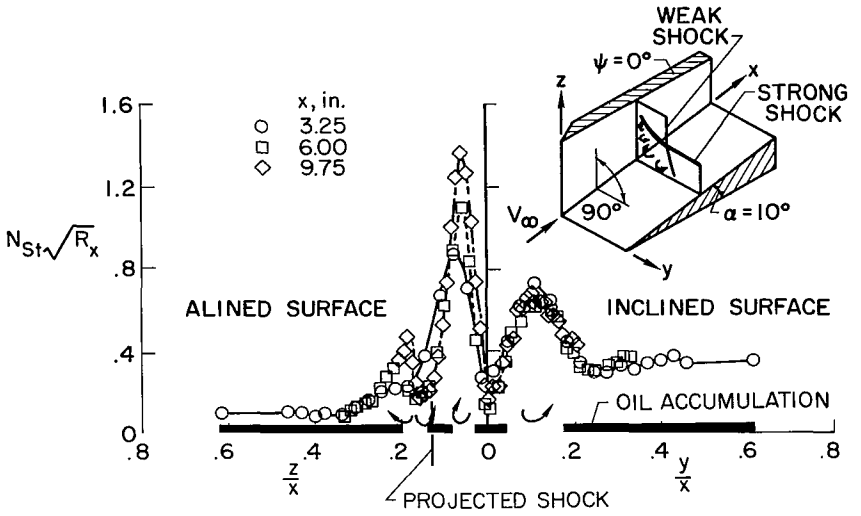

Figure 5.- Heat transfer in a corner. $M_\infty = 8$; $R_\infty/ft = 0.42 \times 10^6$.

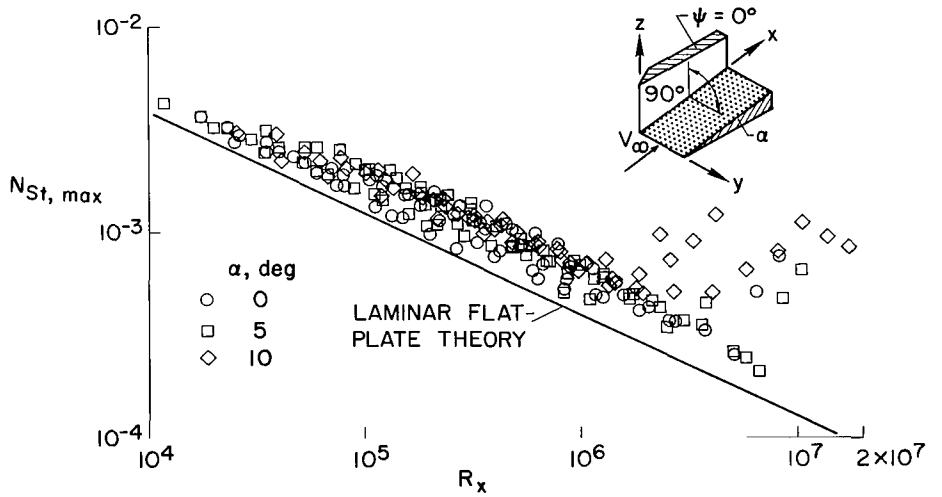

Figure 6.- Laminar peak heating in corner-flow region. Inclined surface; α positive; $M_\infty = 8$; $0.42 \times 10^6 \leqq R_\infty/ft \leqq 10 \times 10^6$.

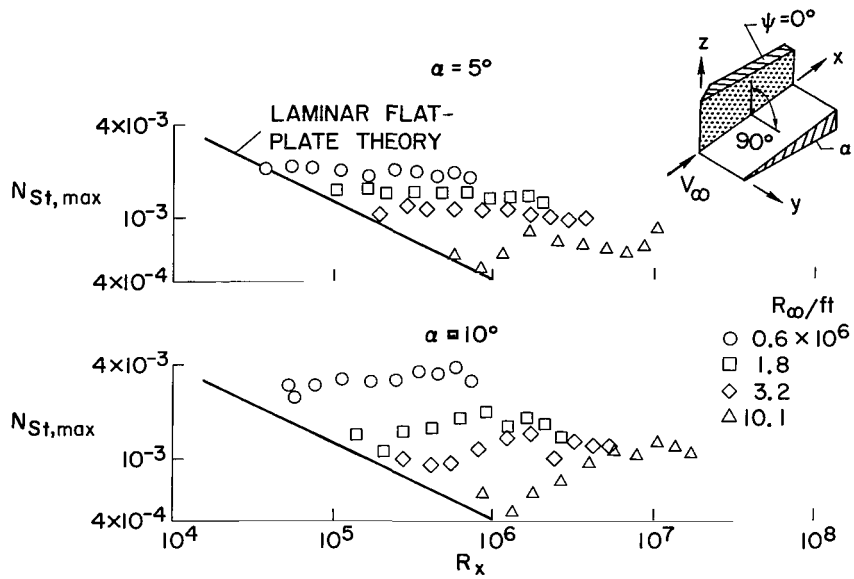

Figure 7.- Laminar peak heating in corner-flow region. Alined surface; α positive; $M_\infty = 8$.

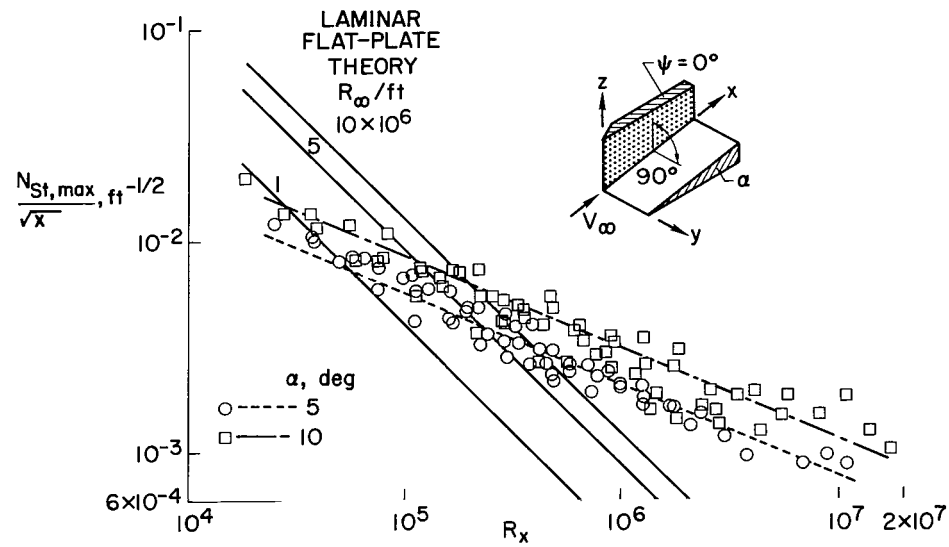

Figure 8.- Laminar peak heating in corner-flow region. Alined surface; α positive; $M_\infty = 8$; $0.42 \times 10^6 \leq R_\infty/\text{ft} \leq 10 \times 10^6$.

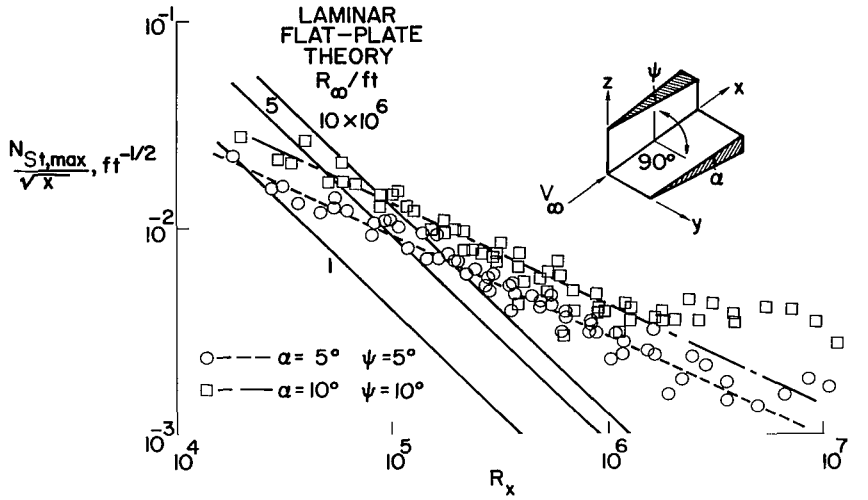

Figure 9.- Laminar peak heating in corner-flow region. α and ψ equal and positive; $M_\infty = 8$; $0.42 \times 10^6 \leqq R_\infty/ft \leqq 10 \times 10^6$.

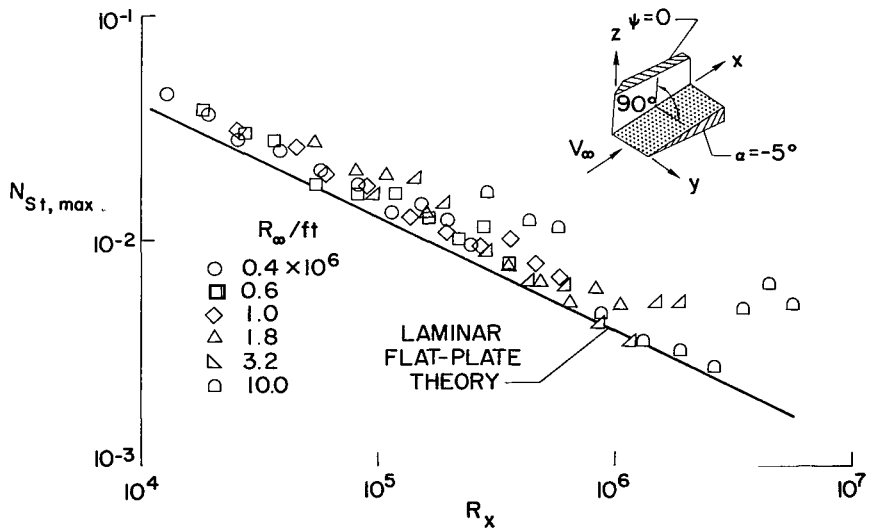

Figure 10.- Laminar peak heating in corner-flow region. Inclined surface; $\alpha = -5°$; $M_\infty = 8$; $0.42 \times 10^6 \leqq R_\infty/ft \leqq 10 \times 10^6$.

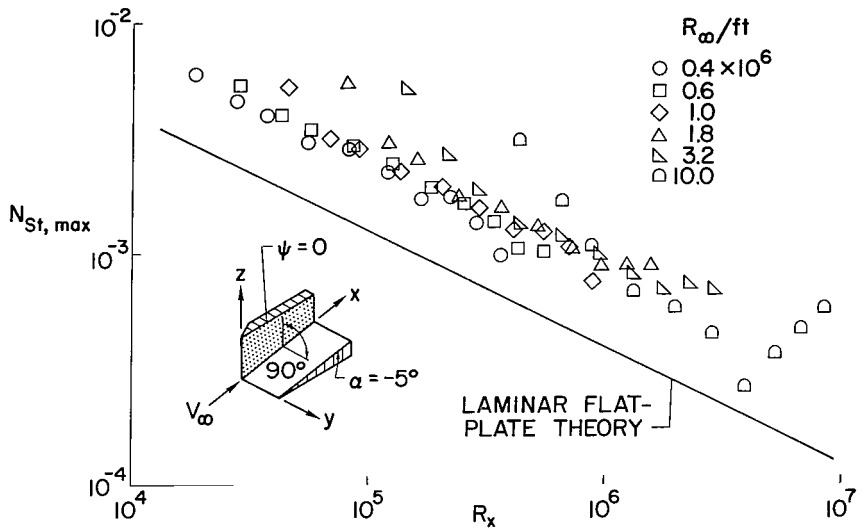

Figure 11.- Laminar peak heating in corner-flow region. Alined surface; $\alpha = -5°$; $M_\infty = 8$; $0.42 \times 10^6 \leqq R_\infty/ft \leqq 10 \times 10^6$.

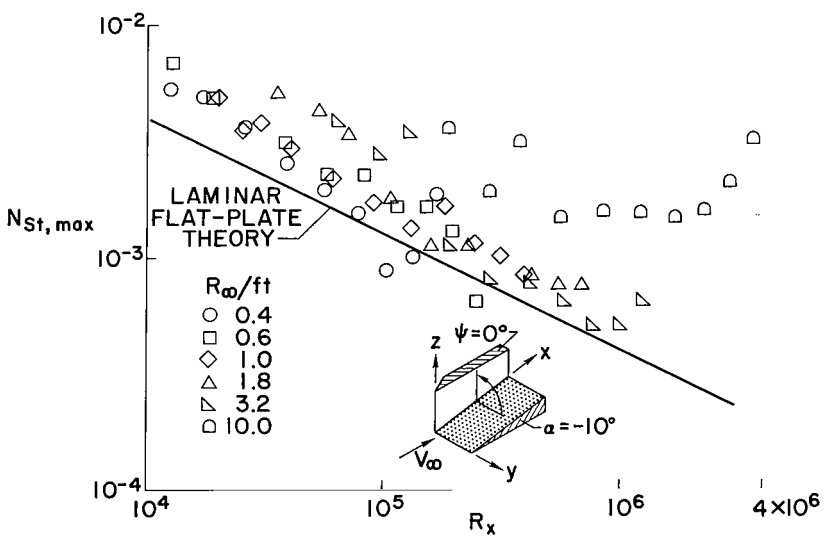

Figure 12.- Laminar peak heating in corner-flow region. Inclined surface; $\alpha = -10°$; $M_\infty = 8$; $0.42 \times 10^6 \leqq R_\infty/ft \leqq 10 \times 10^6$.

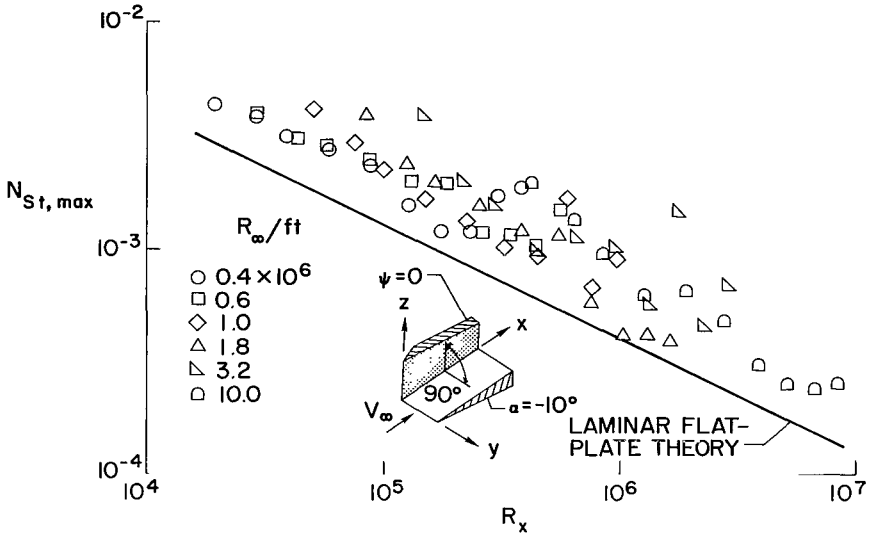

Figure 13.- Laminar peak heating in corner-flow region. Alined surface; $\alpha = -10^\circ$; $M_\infty = 8$; $0.42 \times 10^6 \leqq R_\infty/ft \leqq 10 \times 10^6$.

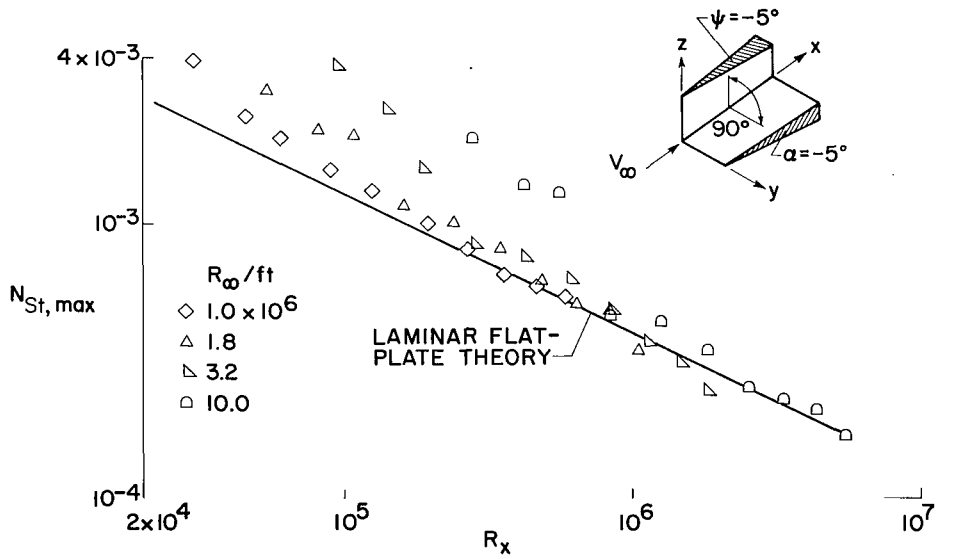

Figure 14.- Laminar peak heating in corner-flow region. α and ψ equal and negative; $M_\infty = 8$; $1 \times 10^6 \leqq R_\infty/ft \leqq 10 \times 10^6$.

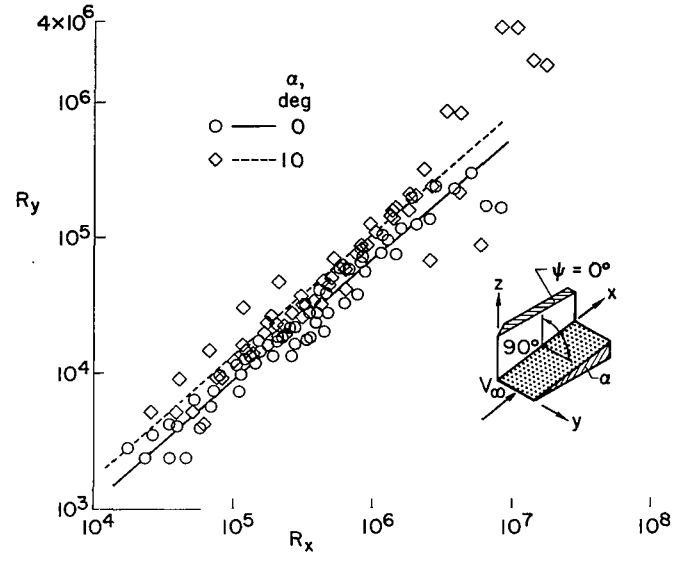

Figure 15.- Location of laminar peak heating. Inclined surface; α positive; $M_\infty = 8$; $0.42 \times 10^6 \leqq R_\infty/\text{ft} \leqq 10 \times 10^6$.

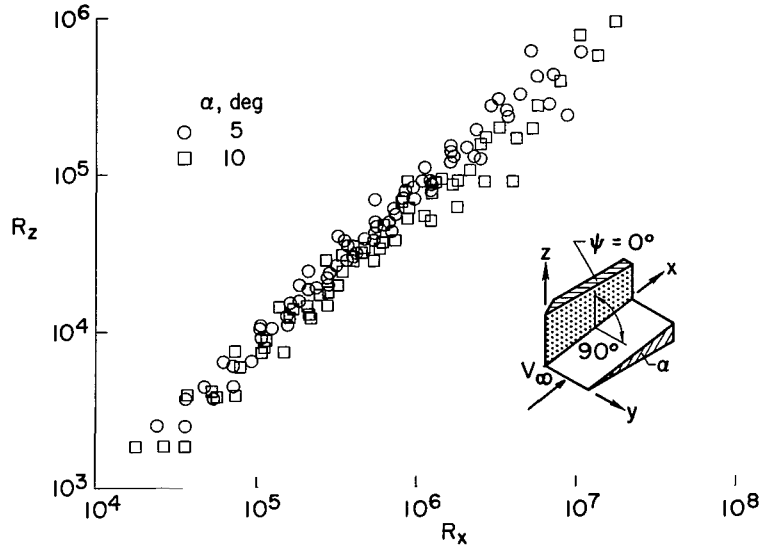

Figure 16.- Location of laminar peak heating. Alined surface; α positive; $M_\infty = 8$; $0.42 \times 10^6 \leqq R_\infty/\text{ft} \leqq 10 \times 10^6$.

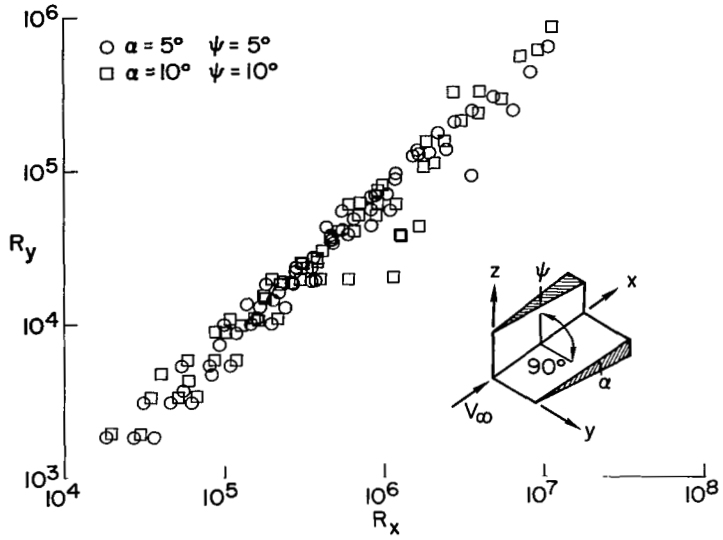

Figure 17.- Location of laminar peak heating. α and ψ equal and positive; $M_\infty = 8$; $0.42 \times 10^6 \leqq R_\infty/ft \leqq 10 \times 10^6$.

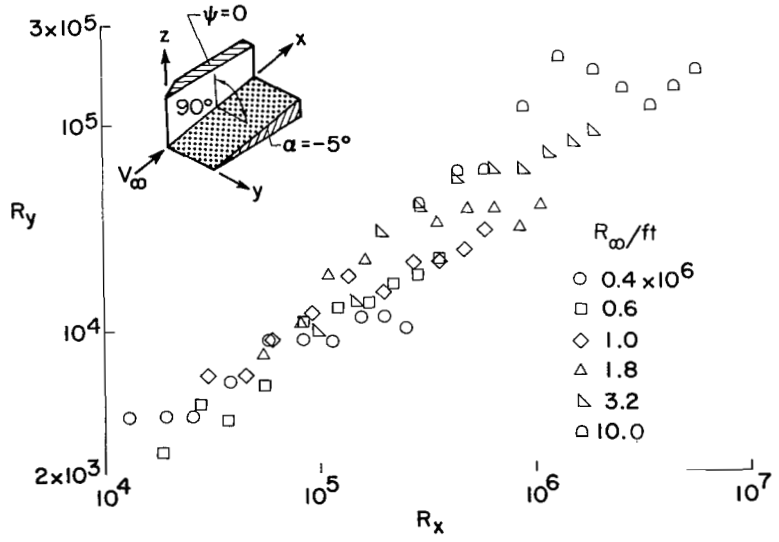

Figure 18.- Location of laminar peak heating. Inclined surface; $\alpha = -5°$; $M_\infty = 8$; $0.42 \times 10^6 \leqq R_\infty/ft \leqq 10 \times 10^6$.

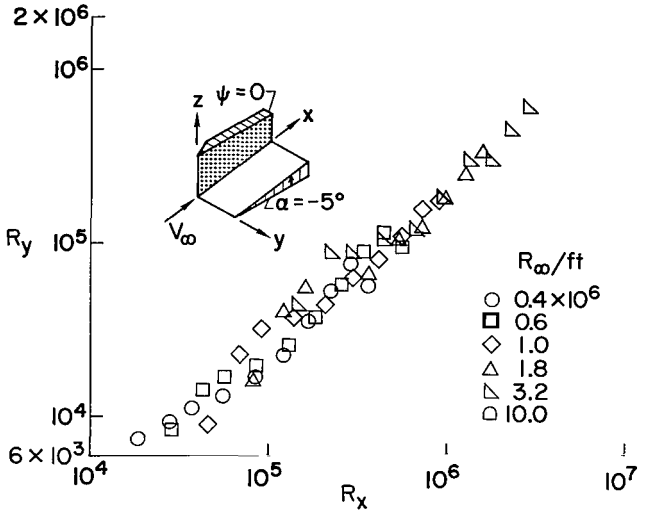

Figure 19.- Location of laminar peak heating. Alined surface; $\alpha = -5^{\circ}$; $M_{\infty} = 8$; $0.42 \times 10^6 \leqq R_{\infty}/ft \leqq 10 \times 10^6$.

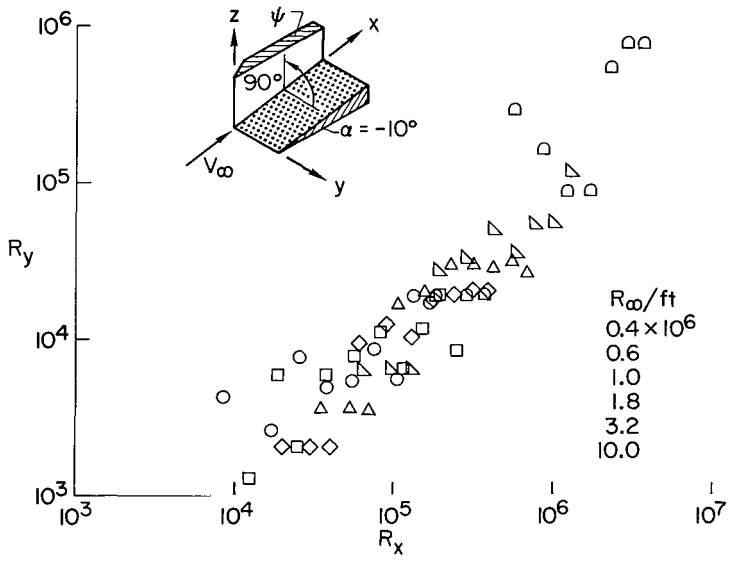

Figure 20.- Location of laminar peak heating. Inclined surface; $\alpha = -10^{\circ}$; $M_{\infty} = 8$; $0.42 \times 10^6 \leqq R_{\infty}/ft \leqq 10 \times 10^6$.

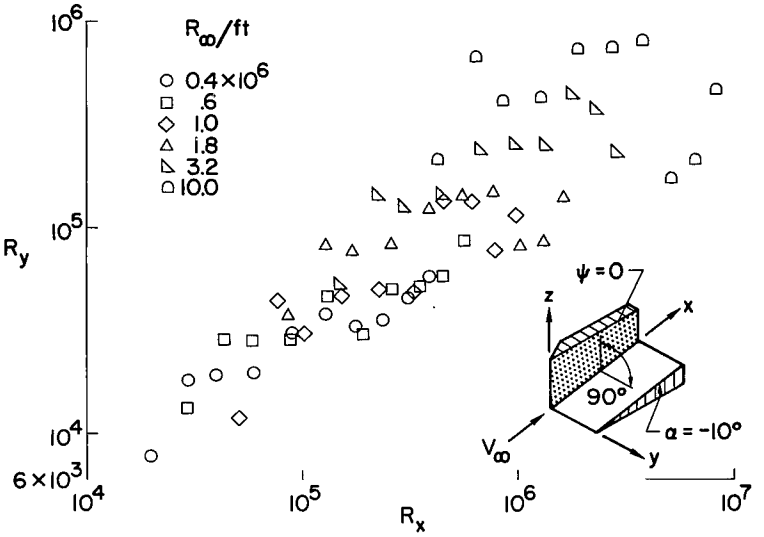

Figure 21.- Location of laminar peak heating. Alined surface; $\alpha = -10^\circ$; $M_\infty = 8$; $0.42 \times 10^6 \leq R_\infty/ft \leq 10 \times 10^6$.

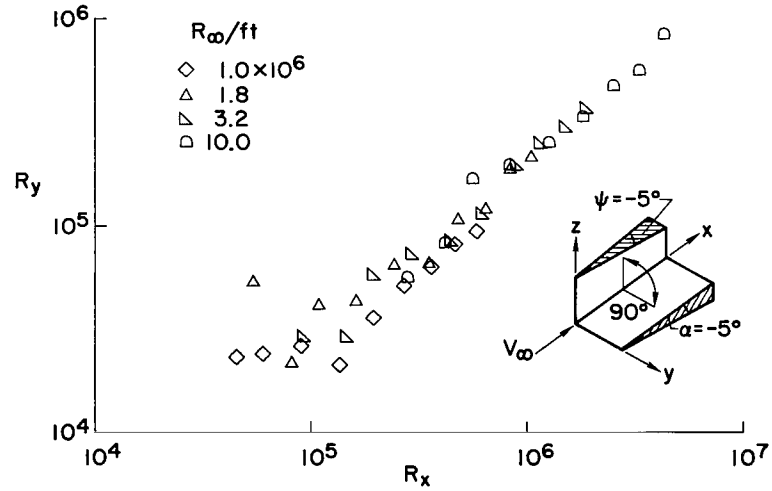

Figure 22.- Location of laminar peak heating. α and ψ equal and negative; $M_\infty = 8$; $1.0 \times 10^6 \leq R_\infty/ft \leq 10 \times 10^6$.

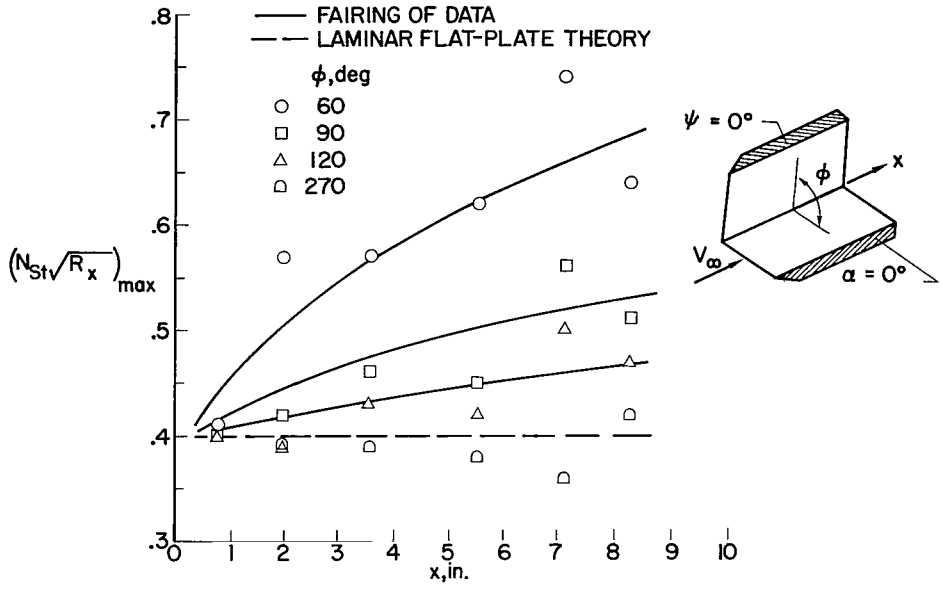

Figure 23.- Effect of cant angle on laminar peak heating. $M_\infty = 8$; $R_\infty/ft = 0.56 \times 10^6$.

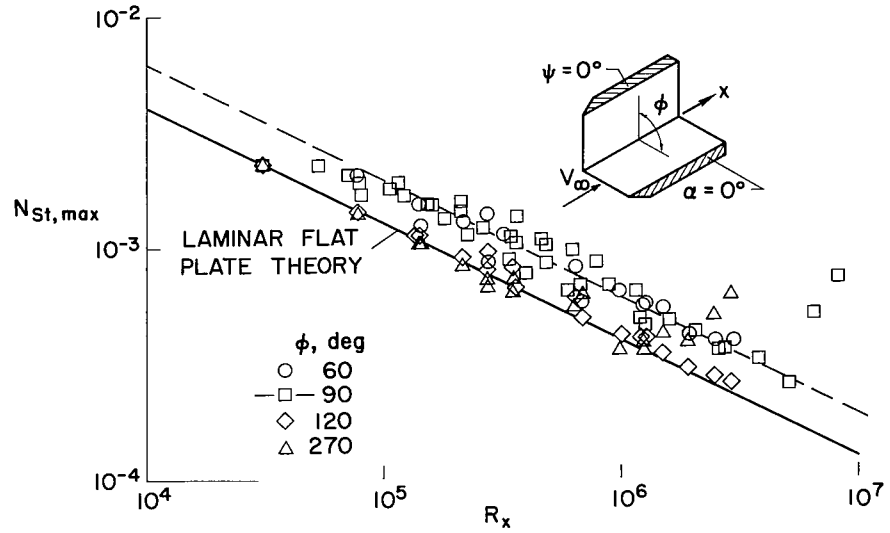

Figure 24.- Effect of cant angle on laminar peak heating. $M_\infty = 8$.

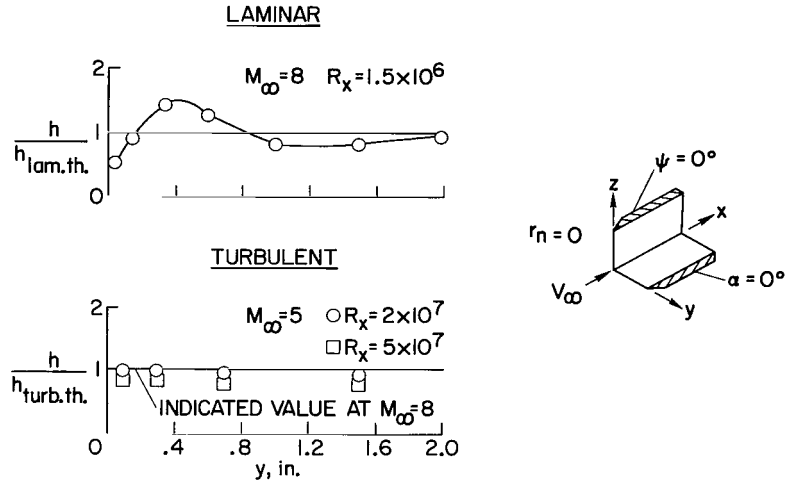

Figure 25.- Comparison of laminar and turbulent heating in a corner; sharp leading edge.

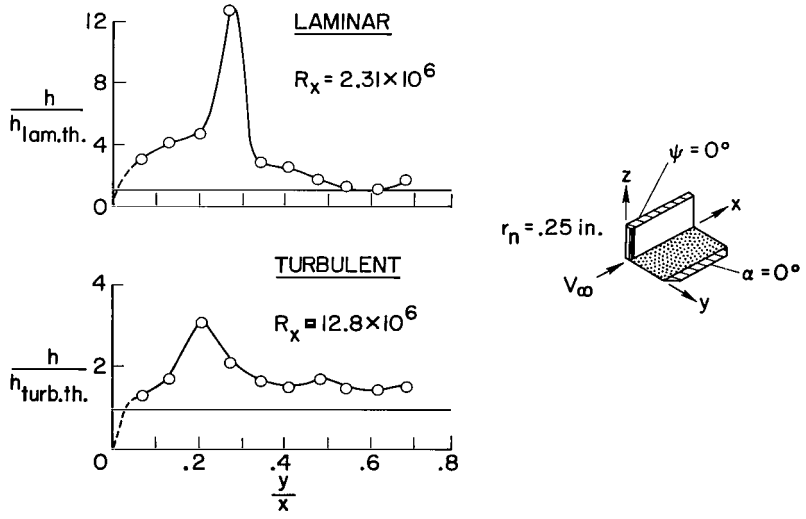

Figure 26.- Comparison of laminar and turbulent heating in a corner; blunt leading edge; $M_\infty = 8$; $\frac{x}{r_n} = 58.2$.

"The aeronautical and space activities of the United States shall be conducted so as to contribute . . . to the expansion of human knowledge of phenomena in the atmosphere and space. The Administration shall provide for the widest practicable and appropriate dissemination of information concerning its activities and the results thereof."

—NATIONAL AERONAUTICS AND SPACE ACT OF 1958

NASA SCIENTIFIC AND TECHNICAL PUBLICATIONS

TECHNICAL REPORTS: Scientific and technical information considered important, complete, and a lasting contribution to existing knowledge.

TECHNICAL NOTES: Information less broad in scope but nevertheless of importance as a contribution to existing knowledge.

TECHNICAL MEMORANDUMS: Information receiving limited distribution because of preliminary data, security classification, or other reasons.

CONTRACTOR REPORTS: Scientific and technical information generated under a NASA contract or grant and considered an important contribution to existing knowledge.

TECHNICAL TRANSLATIONS: Information published in a foreign language considered to merit NASA distribution in English.

SPECIAL PUBLICATIONS: Information derived from or of value to NASA activities. Publications include conference proceedings, monographs, data compilations, handbooks, sourcebooks, and special bibliographies.

TECHNOLOGY UTILIZATION PUBLICATIONS: Information on technology used by NASA that may be of particular interest in commercial and other non-aerospace applications. Publications include Tech Briefs, Technology Utilization Reports and Notes, and Technology Surveys.

Details on the availability of these publications may be obtained from:

SCIENTIFIC AND TECHNICAL INFORMATION DIVISION

NATIONAL AERONAUTICS AND SPACE ADMINISTRATION

Washington, D.C. 20546